

A
QC
807.5
U66
no.
279

NOAA TR ERL 279-OD 9

NOAA Technical Report ERL 279-OD 9

U.S. DEPARTMENT OF COMMERCE
NATIONAL OCEANIC AND ATMOSPHERIC ADMINISTRATION
Environmental Research Laboratories

A Two-Dimensional Theoretical Model for Stratospheric Ozone Density Distributions in the Meridional Plane

T. SHIMAZAKI
D.J. WUEBBLES
T. OGAWA

DULDER, COLO.
AUGUST 1973

ENVIRONMENTAL RESEARCH LABORATORIES

The mission of the Environmental Research Laboratories is to study the oceans, inland waters, the lower and upper atmosphere, the space environment, and the earth, in search of the understanding needed to provide more useful services in improving man's prospects for survival as influenced by the physical environment. Laboratories contributing to these studies are:

Earth Sciences Laboratories (ESL): Seismology, geomagnetism, geodesy, and related earth sciences; earthquake processes, internal structure and shape of the earth and distribution of the earth's mass.

Atlantic Oceanographic and Meteorological Laboratories (AOML): Geology and geophysics of ocean basins, oceanic processes, and sea-air interactions (Miami, Florida).

Pacific Oceanographic Laboratories (POL): Oceanography with emphasis on the oceanic processes and dynamics; tsunami generation, propagation, modification, detection, and monitoring (Seattle, Washington).

Atmospheric Physics and Chemistry Laboratory (APCL): Processes of cloud and precipitation physics; chemical composition and nucleating substances in the lower atmosphere; and laboratory and field experiments toward developing feasible methods of weather modification.

Air Resources Laboratories (ARL): Diffusion, transport, and dissipation of atmospheric contaminants; development of methods for prediction and control of atmospheric pollution; geophysical monitoring for climatic change (Silver Spring, Maryland).

Geophysical Fluid Dynamics Laboratory (GFDL): Dynamics and physics of geophysical fluid systems; development of a theoretical basis, through mathematical modeling and computer simulation, for the behavior and properties of the atmosphere and the oceans (Princeton, New Jersey).

National Severe Storms Laboratory (NSSL): Tornadoes, squall lines, thunderstorms, and other severe local convective phenomena directed toward improved methods of prediction and detection (Norman, Oklahoma).

Space Environment Laboratory (SEL): Solar-terrestrial physics, service and technique development in the areas of environmental monitoring and forecasting.

Aeronomy Laboratory (AL): Theoretical, laboratory, rocket, and satellite studies of the physical and chemical processes controlling the ionosphere and exosphere of the earth and other planets, and of the dynamics of their interactions with high altitude meteorology.

Wave Propagation Laboratory (WPL): Development of new methods for remote sensing of the geophysical environment with special emphasis on optical, microwave and acoustic sensing systems.

Weather Modification Program Office (WMPO): Plans and directs ERL weather modification activities, operates ERL aircraft fleet, and research on cumulus cloud modification, on hurricanes and other tropical problems, and on hurricane modification.

NATIONAL OCEANIC AND ATMOSPHERIC ADMINISTRATION

BOULDER, COLORADO 80302

A
OC
807.5
466
No. 279



U.S. DEPARTMENT OF COMMERCE

Frederick B. Dent, Secretary

NATIONAL OCEANIC AND ATMOSPHERIC ADMINISTRATION

Robert M. White, Administrator

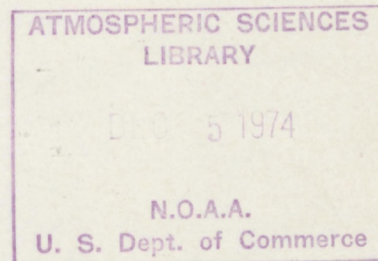
ENVIRONMENTAL RESEARCH LABORATORIES

Wilmot N. Hess, Director

NOAA TECHNICAL REPORT ERL 279-OD 9

A Two-Dimensional Theoretical Model for Stratospheric Ozone Density Distributions in the Meridional Plane

T. SHIMAZAKI
D.J. WUEBBLES
T. OGAWA



BOULDER, COLO.
August 1973

For sale by the Superintendent of Documents, U. S. Government Printing Office, Washington, D. C. 20402

74 5417

TABLE OF CONTENTS

	Page
1. INTRODUCTION	1
2. BASIC EQUATIONS	2
3. METHOD OF NUMERICAL ANALYSIS	5
4. PARAMETERIZATION OF STRATOSPHERIC DYNAMICS	8
4.1 Large Scale Eddy Diffusion	8
4.2 Meridional Circulation	10
5. CHEMICAL REACTIONS	11
6. RESULTS AND DISCUSSIONS	14
6.1 Photochemical Equilibrium Distribution	14
6.2 Effects of Large Scale Eddy Diffusion	16
6.3 Effects of Eddy Diffusion Plus Meridional Circulation	19
7. CONCLUDING REMARKS	24
8. ACKNOWLEDGMENTS	25
9. REFERENCES	25
APPENDIX 1: AN IMPLICIT METHOD FOR THE COLUMN j	27
APPENDIX 2: AN IMPLICIT METHOD FOR THE ROW k (CYCLIC BOUNDARY CONDITION)	28

A TWO-DIMENSIONAL THEORETICAL MODEL FOR STRATOSPHERIC OZONE DENSITY DISTRIBUTIONS IN THE MERIDIONAL PLANE

T. Shimazaki, D. J. Wuebbles and T. Ogawa

It is well known that the photochemical theory is not adequate in explaining many aspects of the observed ozone density distribution in the stratosphere. Both vertical and horizontal transports should play important roles and any model must be at least two dimensional. A time-dependent, two-dimensional model has been developed for the stratospheric ozone density distribution in the 360° meridional domain. The side boundary condition is given by the requirement of the cyclic variation every 360° . In this model the difference between the sunlit-side and dark-side hemisphere, as well as the latitudinal and seasonal variations, can be calculated in a single model calculation. We use an alternating direction implicit line iterative method for solving numerically the two-dimensional continuity equation for the zonal average of the ozone density. Effects of large scale eddy diffusion and meridional circulation are introduced by parameterization, respectively, in terms of the effective eddy diffusion coefficients and three cell motions in each of the sunlit-side and dark-side hemispheres. These two effects tend to cancel each other to some extent, but the result of the present study indicates that a proper combination of these two dynamics can explain well the discrepancies between the photochemical model and the observations on the global distribution of the ozone density.

1. INTRODUCTION

It has been well recognized that the distributions of minor neutral constituents in the stratosphere, especially ozone, play an important role in the global energy budget and radiation balance in the atmosphere. While comprising only 3×10^{-7} of the atmosphere, the stratospheric ozone strongly absorbs solar ultraviolet radiation and provides the principal heat energy in the atmosphere.

The ozone density in the stratosphere is determined mainly by photochemical reactions, i.e., by the balance between the production due to three-body recombination of O and O₂ and the destruction by the ozone photolysis. It is well established, however, that a realistic model of the stratospheric ozone density distribution can not be obtained on the assumption of photochemical equilibrium. If the time to reach photochemical equilibrium is more than a day or so for an atmospheric constituent, transport effects become important in determining the distribution of that constituent.

For ozone in the stratosphere, the time to reach equilibrium increases from less than a day at the stratopause to more than a year in the lower stratosphere (Dütsch, 1961; Nicolet, 1972). Therefore, below approximately 45 km atmospheric dynamics become increasingly important.

Prabhakara (1963) has shown that the addition of dynamics in a meridional model of the ozone layer gets much closer to the observed ozone density distributions than the model of photochemical equilibrium can predict. Hesstvedt (1972) has added water vapor and nitrogen chemistry to the Prabhakara's model. Because their domain was either 180° or 90° meridional plane, however, they had to postulate side boundary conditions, which were not necessarily reasonable. For a model of global scale, it would be better to consider the entire region of the atmosphere as a domain. Then, the side boundary condition can be given in a more reasonable form, i.e., it requires that any variable take the same value every 360° in the meridional plane.

For a general circulation model of the mean atmosphere, horizontal motions are primarily important, and vertical motions are of only secondary importance. For determining the height distributions of the chemically active minor constituents, however, vertical transports are essentially important because sources and sinks are strongly height dependent. For the stratospheric ozone, both vertical and horizontal transport should be important, and must be included in any model of that region; therefore, any model should be at least two-dimensional.

In this paper we describe the modeling technique of our time-dependent two-dimensional model in the 360° meridional plane. The effects of large scale eddy diffusion and meridional circulation, as well as the ozone chemistry in the pure oxygen atmosphere, have been incorporated into the model. It is proven from a preliminary result presented here that the model can explain well the observed features of the world-wide distributions of the stratospheric ozone density.

2. BASIC EQUATIONS

It would be ideal for the numerical modeling of the stratosphere to solve the thermodynamic equation and the equations of motion simultaneously with continuity equations for various constituents in the three dimensional domain. The development of a three dimensional, global circulation model with fully interactive chemistry, fluid dynamics, and thermodynamics, however, requires an enormous amount of computer time and man power. For the stratospheric ozone problem, a less comprehensive, simplified model may solve the problem to some extent without requiring the large amount of computer time needed by the global circulation models.

We have developed a two-dimensional time-dependent model for the stratosphere by extending our previously developed one-dimensional models for the mesosphere and lower thermosphere (Shimazaki, 1967 and 1972; Shimazaki and Laird, 1970 and 1972). In our two dimensional domain, the meridional plane of 360° is considered for the height range of 10 to 50 km,

comprising most of the stratosphere, for each 10° of latitude. By using the 360° meridional plane we can set a side boundary condition requiring the cyclic variation every 360° , which is more reasonable than the zero-flux or based-on-observation boundary conditions in some of the two-dimensional models of 180° or 90° domain. As is seen in figure 1, which shows the meridional plane used in this study with the sun being at an angle δ from the equator, our model has another advantage in the sense that the difference between the sunlit and dark side hemisphere, as well as the seasonal and latitudinal variations, can be calculated in one model calculation.

We solve the zonally averaged continuity equations for various constituents in the meridional plane, assuming the thermal and dynamical

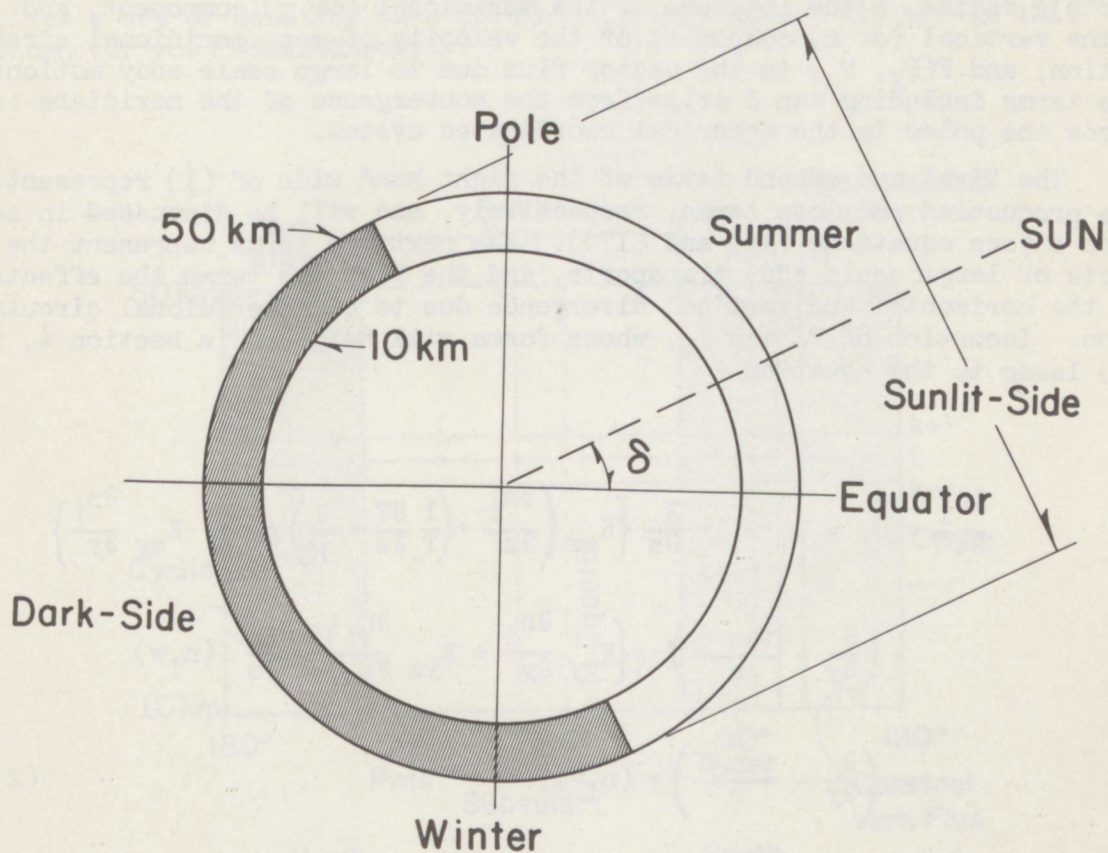


Figure 1. 360° meridional plane as used in our model calculation.

structure based on observations and theoretical estimates. The equation can be written as

$$\begin{aligned}
 \frac{\partial n_i}{\partial t} = & Q_i - L_i \cdot n_i - \left(\frac{\partial}{\partial y} - \frac{\tan \theta}{r} \right) \cdot F_y \\
 & - \frac{\partial}{\partial z} F_z - \left(\frac{\partial}{\partial y} - \frac{\tan \theta}{r} \right) \cdot (n_i v) \\
 & - \frac{\partial}{\partial z} (n_i w) \tag{1}
 \end{aligned}$$

where n_i is the number density of the i^{th} constituent, t the time, r the earth's radius, θ the latitude, v the meridional (or y) component, and w the vertical (or z) component of the velocity of mean meridional circulation, and $F(F_y, F_z)$ is the vector flux due to large scale eddy motions. The terms including $\tan \theta$ arise from the convergence of the meridians towards the poles in the spherical coordinates system.

The first and second terms of the right hand side of (1) represent the production and loss terms, respectively, and will be discussed in section 5 (see equations (16) and (17)). The next two terms represent the effects of large scale eddy transports, and the last two terms the effects of the horizontal and vertical divergence due to mean meridional circulation. Insertion of F_y and F_z , whose forms will be given in section 4, into (1) leads to the equation

$$\begin{aligned}
 \frac{\partial n_i}{\partial t} = & Q_i - L_i \cdot n_i + \frac{\partial}{\partial z} \left\{ K_{zz} \left(\frac{\partial n_i}{\partial z} + \left(\frac{1}{T} \frac{\partial T}{\partial z} + \frac{1}{H} \right) n_i \right) + K_{zy} \frac{\partial n_i}{\partial y} \right\} \\
 & + \left(\frac{\partial}{\partial y} - \frac{\tan \theta}{r} \right) \cdot \left\{ K_{yy} \frac{\partial n_i}{\partial y} + K_{yz} \frac{\partial n_i}{\partial z} \right\} - \frac{\partial}{\partial z} (n_i w) \\
 & - \left(\frac{\partial}{\partial y} - \frac{\tan \theta}{r} \right) \cdot (n_i v). \tag{2}
 \end{aligned}$$

This is the equation we solve in the next section. The explanation for T , H , and K 's will be given in section 4 (see equations (11) and (12)).

3. METHOD OF NUMERICAL ANALYSIS

The grid used in representing our two-dimensional stratospheric model is shown in figure 2. At each grid point the continuity equation (2) can be written in a form of the finite difference equation, in which $n_i(j,k)$ is related to the values at the four adjacent points, i.e., $n_i(j-1,k)$, $n_i(j+1,k)$, $n_i(j,k+1)$ and $n_i(j,k-1)$, where j and k are the indicators of the grid points in the y - and z - directions, respectively. They take the numbers of $1,2,3,\dots,J$ and $1,2,3,\dots,K$, respectively.

In solving these finite difference equations the so-called implicit method is known to give faster and better convergency than the explicit method (Richtmyer and Morton, 1967). The implicit method solves a set of equations for all n_i 's simultaneously, whereas the explicit method solves each equation for n_i separately. Details of the method has been explained in Shimazaki (1967) for the case of one-dimensional modeling. Extending this technique to two-dimensional modeling is not possible in a strict sense, but a somewhat analogous method, i.e., the implicit line iterative method (see, for example, Young, 1962) may be useful. Instead of solving all equations for $n(j,k)$ simultaneously, the method solves a set of equation in a column j (or row k) for all n 's in that column (or row) simultaneously.

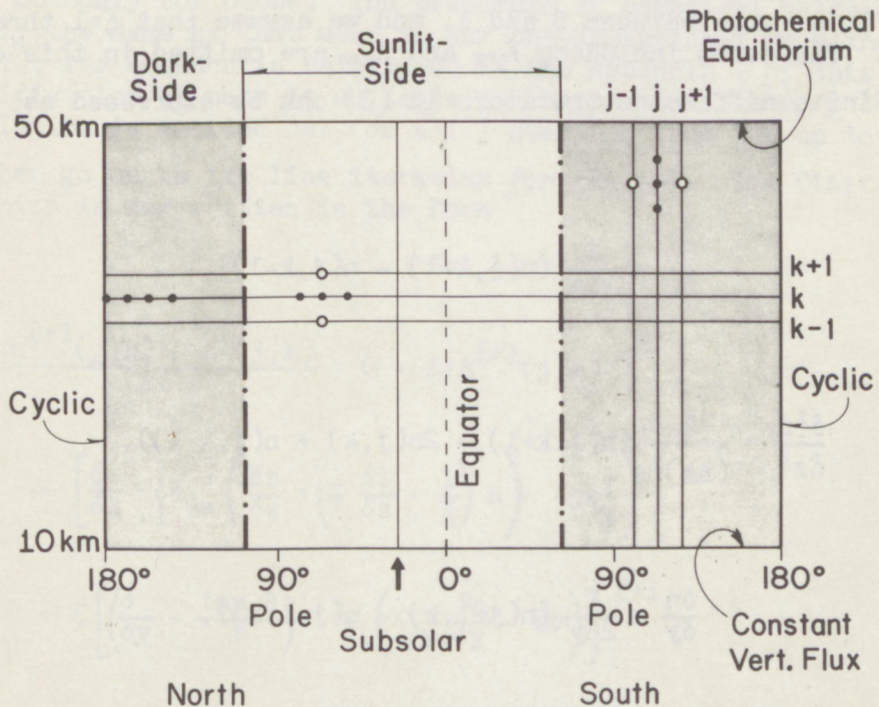


Figure 2. Grid used in representing the stratosphere.

We first consider a line iteration *for the column*. The finite difference equation (2) in column j and row k can be written as (we omit the subscript i)

$$\begin{aligned}
 \frac{n^{\ell+1}(j,k) - n^{\ell}(j,k)}{\Delta t} &= Q - L \cdot n^{\ell+1}(j,k) \\
 &+ \xi \left[\frac{\delta}{\delta z} \left\{ K_{zz} \left(\frac{\delta n}{\delta z} + \left(\frac{1}{T} \frac{\delta T}{\delta z} + \frac{1}{H} \right) n \right) - nw \right\} \right]^{\ell+1} \\
 &+ (1-\xi) \left[\frac{\delta}{\delta z} \left\{ K_{zz} \left(\frac{\delta n}{\delta z} + \left(\frac{1}{T} \frac{\delta T}{\delta z} + \frac{1}{H} \right) n \right) - nw \right\} \right]^{\ell} \\
 &+ \left[\left(\frac{\delta}{\delta y} - \frac{\tan \theta}{r} \right) \cdot \left(K_{yy} \frac{\delta n}{\delta y} - nv \right) \right]^{\ell} \tag{3}
 \end{aligned}$$

where the superscript ℓ and $\ell+1$ indicate, respectively, the values at the time ℓ and the time $\ell+1$, and δ represents the finite difference. ξ is a parameter in a range between 0 and 1, and we assume that $\xi=1$ throughout the study. The terms including K_{yz} and K_{zy} are omitted in this expression.

The finite difference operators in (3) can be expressed as

$$\frac{\delta n}{\delta z} = \frac{1}{2\Delta z} \{n(j,k+1) - n(j,k-1)\}, \tag{4}$$

$$\frac{\delta^2 n}{\delta z^2} = \frac{1}{(\Delta z)^2} \{n(j,k+1) - 2n(j,k) + n(j,k-1)\}, \tag{5}$$

$$\frac{\delta n}{\delta y} = \frac{1}{2\Delta y} \{n(j+1,k) - n(j-1,k)\}, \tag{6}$$

$$\frac{\delta^2 n}{\delta y^2} = \frac{1}{(\Delta y)^2} \{n(j+1,k) - 2n(j,k) + n(j-1,k)\}, \tag{7}$$

where Δy and Δz represent the increments in the meridional and vertical direction, respectively. Because of the cyclic boundary condition, we have

$$n(0,k) = n(J-1,k) \text{ and } n(J,k) = n(1,k). \quad (8)$$

Inserting equations (4) through (7) into (3), we find that the equation includes five values of n , of which three variables appearing in (4) and (5) and $n(j,k)^{\ell+1}$ in the left hand side and in the loss term of (3) are considered to be the values at the time $\ell+1$ and therefore unknowns. The rest of n are taken from the known values at the previous time step (or at the time ℓ), or if the line iteration for the column starts from $j=1$ and proceeds to the increasing value for j , $n(j-1,k)$ may be taken from the result of the previous line iteration at the time $\ell+1$. The three unknown variables are shown by filled-in circles in the column j and the known variables by the white circles in the column $j+1$ or $j-1$ in figure 2.

Equation (3) can be written for $k = 2, 3, 4, \dots$, and $K-1$ and these $K-2$ equations include K unknowns, i.e., the values of n at $k = 1, 2, 3, \dots$, and K in the column j ; therefore, two more equations are needed to solve a set of equations simultaneously for all n 's in the column j , and these are supplied by the upper and lower boundary conditions. We assume photochemical equilibrium at the upper boundary and a constant flux with height at the lower boundary for ozone. The procedure of numerical calculation is essentially the same as that used in our one-dimensional modeling (Shimazaki, 1967); its essence is reiterated in the Appendix 1 of this paper after modification to make it suitable to the present boundary conditions. The calculation is carried out for all j starting from $j=1$ up to $j=J-1$.

We then go on to the line iteration *for the row*. The finite difference equation is now written in the form

$$\begin{aligned} \frac{n^{\ell+1}(j,k) - n^{\ell}(j,k)}{\Delta t} &= Q - L \cdot n^{\ell+1}(j,k) \\ &+ \left[\frac{\delta}{\delta z} \left\{ K_{zz} \left(\frac{\delta n}{\delta z} + \left(\frac{1}{T} \frac{\delta T}{\delta z} + \frac{1}{H} \right) n \right) - nw \right\} \right]^{\ell} \\ &+ \xi \left[\left(\frac{\delta}{\delta y} - \frac{\tan \theta}{r} \right) \cdot \left(K_{yy} \frac{\delta n}{\delta y} - nv \right) \right]^{\ell+1} \\ &+ (1-\xi) \cdot \left[\left(\frac{\delta}{\delta y} - \frac{\tan \theta}{r} \right) \cdot \left(K_{yy} \frac{\delta n}{\delta y} - nv \right) \right]^{\ell} \end{aligned} \quad (9)$$

Inserting equations (4) through (7) into (9) gives us the equation including five n , of which the three variables appearing in (6) and (7) and $n^{l+1}(j,k)$ in the left hand side and in the loss term of (9) are considered to be unknowns. Thus, (9) has three unknown variables $n(j+1,k)$, $n(j,k)$ and $n(j-1,k)$ in the row of k . The other n 's in (9) are taken from either the result of previous iteration for the row of $k+1$ or the result of previous time step for the row of $k-1$. Note that we start the line iteration for the row from the top, i.e., $k = K-1$ and go down to $k=1$.

Equation (9) written for $j=1$ needs the variable at $j=0$, as is seen in (6) and (7), but that can be replaced by the variable at $j = J-1$ by the condition of cyclic variation (see (8)), and similarly, equation (9) written for $j = J-1$ need the variable at $j=J$ as is seen in (4) and (5), but this can be replaced by the variable at $j=1$. Consequently, we have $J-1$ independent equations for $J-1$ unknowns, i.e., the values of n at $j = 1, 2, 3, \dots$, and $J-1$ in the row of k . Thus, a set of equations is now ready for solving. Actually, we have developed a special technique to solve this problem effectively (see Appendix 2).

We repeat the calculations by the abovementioned method for the column and the row alternatively until we get the satisfactory convergence for the solution. The method is then called the alternating direction implicit line iterative method (Young, 1972).

4. PARAMETERIZATION OF STRATOSPHERIC DYNAMICS

In our parameterized modeling, values of temperature, eddy diffusion coefficients, and mean meridional circulation are assumed based on observations and theoretical estimates.

Details about atmospheric motion, particularly in various scales of motion and in time variability of these motions, are difficult to represent; however, it appears that the mean transports of minor neutral constituents in the stratosphere is dominated by large scale motions that can be represented in terms of mean motion (or wind) and eddy (or turbulent) diffusion. The accuracy of these parameterizations in representing the stratospheric dynamics rely heavily on observational data and good theoretical estimates, the amount and quality of which are quite limited at the present.

4.1 Large Scale Eddy Diffusion

A useful method of treating the eddy diffusion flux is to write it in the form

$$\overline{v_i' v_i'} = -K \text{grad } \bar{v}_i, \quad (10)$$

where v_i' represents the fluctuation of v_i , the mixing ratio of the i^{th} constituent, accompanying the random component (v_i') of the velocity, the upper bar indicates the time average, and K is an effective coefficient for eddy diffusivity and is analogous to a molecular diffusivity.

K generally represents an anisotropic eddy diffusion coefficient, and in the two-dimensional model composed of the meridional (y coordinate) and vertical (z coordinate) plane the eddy diffusion flux can be written as

$$F_y = -K_{yy} \frac{\partial n_i}{\partial y} - K_{yz} \frac{\partial n_i}{\partial z} \quad (11)$$

and

$$F_z = -K_{zy} \frac{\partial n_i}{\partial y} - K_{zz} \cdot \left\{ \frac{\partial n_i}{\partial z} + \left(\frac{1}{T} \frac{\partial T}{\partial z} + \frac{1}{H} \right) n_i \right\}, \quad (12)$$

where T is the atmospheric temperature, \bar{H} the scale height of the completely mixed atmosphere, and it is usually assumed that $K_{yz}=K_{zy}$. In some previous studies for minor constituents distributions, for instance, for random (Jacobi and André, 1963)

$$F_z = -K_{zy} \frac{\partial n_i}{\partial y} - K_{zz} \frac{\partial n_i}{\partial y} \quad (13)$$

has been used instead of (12) for representing the vertical flux.

Equation (12) includes the effect of the gravitational field and represents the vertical eddy diffusion flux of the minor constituent through the major constituent, whose density decreases with height by the scale height \bar{H} . If the minor constituent n_i has the same height variation as the major constituent, the mixing ratio of that minor constituent is constant with height, and apparently there is no net vertical diffusion flux for n_i . (We neglect the term of K_{zy} in this discussion.) The similar discussion based on (13) leads to the conclusion that the vertical diffusion flux becomes zero when n_i is constant with height. This is certainly incorrect, since such a distribution of n_i should cause a large downward motion (or flux) because of the gravitational force; thus, it is essential to use (12) instead of (13) in model calculation for minor constituents.

Measurements based on the dispersion of particle trajectories suggest that the order of K_{zz} is 10^3 - 10^4 $\text{cm}^2\text{sec}^{-1}$, K_{yy} 10^9 - 10^{10} $\text{cm}^2\text{sec}^{-1}$, and K_{yz}

(or K_{yz}) $\pm 10^6$ - 10^7 cm²sec⁻¹. The negative value of K_{yz} (or K_{zy}) may occur, when the poleward motion has a greater downward slope than the slope of the isentropes. This is not uncommon in the lower stratosphere (Reed and German, 1965). There are general tendencies that K_{yy} is larger at higher latitudes than at lower latitudes particularly in winter and that K_{zz} decreases with height except for the upper stratosphere, where K_{zz} tends to increase with height.

Reed and German (1965) has calculated K's for every 10° of latitude and at three chosen heights using the heat flux and temperature data. Gudiksen et al. (1968) has applied these results to the calculation of the roles of eddy mixing and mean circulation in determining the spread of tungsten 185 injected into the lower stratosphere from Hardtack test series and have found that the observed distribution of tungsten is reproduced satisfactorily, if the diffusion coefficients estimated from heat flux data are reduced by a factor of about 8. The mean circulation was found to play a minor role in their result.

There are some problems in applying the eddy diffusion coefficients determined by heat flux data to the diffusion of particles (minor constituents) in the stratosphere. The treatment of the anisotropic eddy diffusion in the numerical modeling is certainly complicated, and we have had negative values for n_i at some heights near the lower boundary at some latitudes because of the negative values of K_{yz} (or K_{zy}). It is not certain at this time whether this was caused by the inappropriateness of the assumed values of K_{yz} or by the improper treatment for the numerical analysis. In the present model calculation, we have decided to use the as-simple-as-possible forms for K's; K_{yz} and K_{zy} are assumed to be zero, and cases of constant K_{yy} and K_{zz} have been considered.

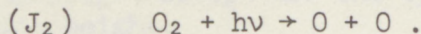
4.2 Meridional Circulation

Mean meridional and vertical motions are important in the transport of heat and momentum and contribute to the movement of trace substances in the stratosphere. Meridional circulations in the stratosphere should play an important role for the ozone density distributions, but it is very difficult to observe them directly; therefore, it is necessary to have good theoretical estimates on the meridional and vertical components of the mean velocity.

Vincent (1968) has calculated mean meridional circulation from zonally-averaged sources and sinks of momentum and heat. The results of the computed velocity components show the flow patterns of cell-like structures. Two large scale cell motions are produced by upward motions over low and middle latitudes in summer hemisphere and downward motions over the summer pole and middle latitudes in winter hemisphere. Additional smaller but not weaker cell motion is developed over the winter hemisphere, having upward motions over the pole and downward motions over middle latitudes.

The intensities and locations of these cells may vary from day to day and from month to month, and it is not appropriate to consider these changes

In this and the following chemical equations, the reactions are shown by k_i for chemical reactions and by J_i for photodissociations; they also represent the reaction or dissociation coefficients. The atomic oxygen needed for k_2 is supplied by photodissociation of O_2



In the upper stratosphere, the Herzberg continuum (2000-2400 Å) is the main source for J_2 , but our model also includes the dissociation at Schumann-Runge bands at 1750-2050 Å (Hudson, 1969), which may dominate over the dissociation at the Herzberg continuum in the lower stratosphere.

Ozone is destroyed by photodissociation



at Hartley bands (2000-3200 Å), Huggins bands (3200-3600 Å), and Chappius bands (4000-8000 Å).

The dissociation coefficient can be calculated by

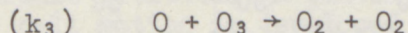
$$J_i = \phi_i \int I(\lambda, z) \alpha_i(\lambda, z) d\lambda$$

where ϕ_i is the quantum yields for photodissociation, α_i is the respective absorption cross-section, and I is the intensity of solar radiation as a function of wavelength λ and the height z . I is given by

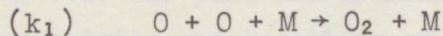
$$I = I_\infty \exp \left(- \sum_j \int n_j \alpha_j \sec \chi dz \right), \quad (15)$$

where I_∞ indicates the intensity of solar radiation at the top of the atmosphere and χ is the incident solar zenith angle.

The odd oxygens are also destroyed by



and



but the reaction k_1 can be neglected in the stratosphere.

Based on the above chemical reaction scheme, the rate equations for [O] and [O₃] can be written as

$$\frac{\partial [O]}{\partial t} = 2 J_2 \cdot [O_2] + J_3 \cdot [O_3] - k_2 \cdot [O] \cdot [O_2] \cdot [M] - k_3 \cdot [O] \cdot [O_3] \quad (16)$$

and

$$\frac{\partial [O_3]}{\partial t} = k_2 \cdot [O] \cdot [O_2] \cdot [M] - k_3 \cdot [O] \cdot [O_3] - J_3 \cdot [O_3]. \quad (17)$$

The right hand side of these equations give the expressions for the chemical reaction terms ($Q_i - L_i n_i$) in the continuity equation (1) and succeeding equations.

Since the chemical time constant for O is very small in the stratosphere, it always is in photochemical equilibrium, and we obtain from (16) by setting $\partial [O] / \partial t = 0$ the following:

$$[O] = \frac{2 J_2 \cdot [O_2] + J_3 \cdot [O_3]}{k_3 \cdot [O_3] + k_2 \cdot [O_2] \cdot [M]}. \quad (18)$$

Inserting (18) into (17) we obtain

$$\frac{\partial [O_3]}{\partial t} = \frac{2 J_2 \cdot [O_2] \cdot (k_2 \cdot [O_2] \cdot [M] - k_3 \cdot [O_3]) - 2 J_3 k_3 [O_3]^2}{k_2 \cdot [O_2] [M] + k_3 [O_3]}, \quad (19)$$

which becomes, on the ground that $k_3 \cdot [O_3] \ll k_2 \cdot [O_2] \cdot [M]$ in the stratosphere,

$$\frac{\partial [O_3]}{\partial t} = 2 J_2 [O_2] - 2 \frac{J_3 \cdot (k_3 / k_2)}{[O_2] [M]} [O_3]^2. \quad (20)$$

In the actual calculation the non-linear term in (20) is linearized by the approximation based on the Taylor expansion as follows:

$$[O_3]_{t+1}^2 = [O_3]_t^2 + 2[O_3]_t([O_3]_{t+1} - [O_3]_t) = 2[O_3]_t[O_3]_{t+1} - [O_3]_t^2, \quad (21)$$

and the equation (20) has been solved by including transport terms.

Since our model includes the dark-side hemisphere, it is essential to solve the *time-dependent* continuity equation for $[O_3]$. All terms in the right hand side of (17) vanish in the dark-side hemisphere, since there is no photodissociation and $[O]$ is zero based on (18); therefore, for steady state $[O_3]$ must be determined by the condition of $\text{div}([O_3] \cdot v) = 0$, which gives a very strange distribution for $[O_3]$. Note that we do not rotate the earth and therefore do not calculate the diurnal variation. We calculate how the ozone density distribution changes if the sunlit or dark condition continues for a long time.

The initial condition for $[O_3]$ distribution in the sunlit-side hemisphere is given by the photochemical equilibrium. Combining (17) and (18) after setting $\partial[O_3]/\partial t = 0$, we obtain a quadratic equation for $[O_3]$

$$J_3 \cdot k_3 [O_3]^2 + J_2 \cdot k_3 \cdot [O_2] \cdot [O_3] - J_2 \cdot k_2 \cdot [O_2]^2 \cdot [M] = 0 \quad (22)$$

whose solution is given by

$$[O_3] = \frac{-J_2 + \sqrt{J_2^2 + 4 J_2 \cdot J_3 \cdot (k_2/k_3) \cdot [M]}}{2 J_3} [O_2]. \quad (23)$$

In the dark-side hemisphere the initial condition is assumed to be the same as that calculated by (23) for the sunlit-side hemisphere for the corresponding latitude. While the chemical source and sink continue to exist in the sunlit-side hemisphere, they disappear immediately after $t = 0$ in the darkside hemisphere.

6. RESULTS AND DISCUSSIONS

6.1 Photochemical Equilibrium Distribution

We first calculate the photochemical equilibrium distributions for $[O_3]$ and $[O]$ by (23) and (18), respectively. The temperature structure is assumed, as is shown in figure 4, based on Murgatroyd (1967). The solar

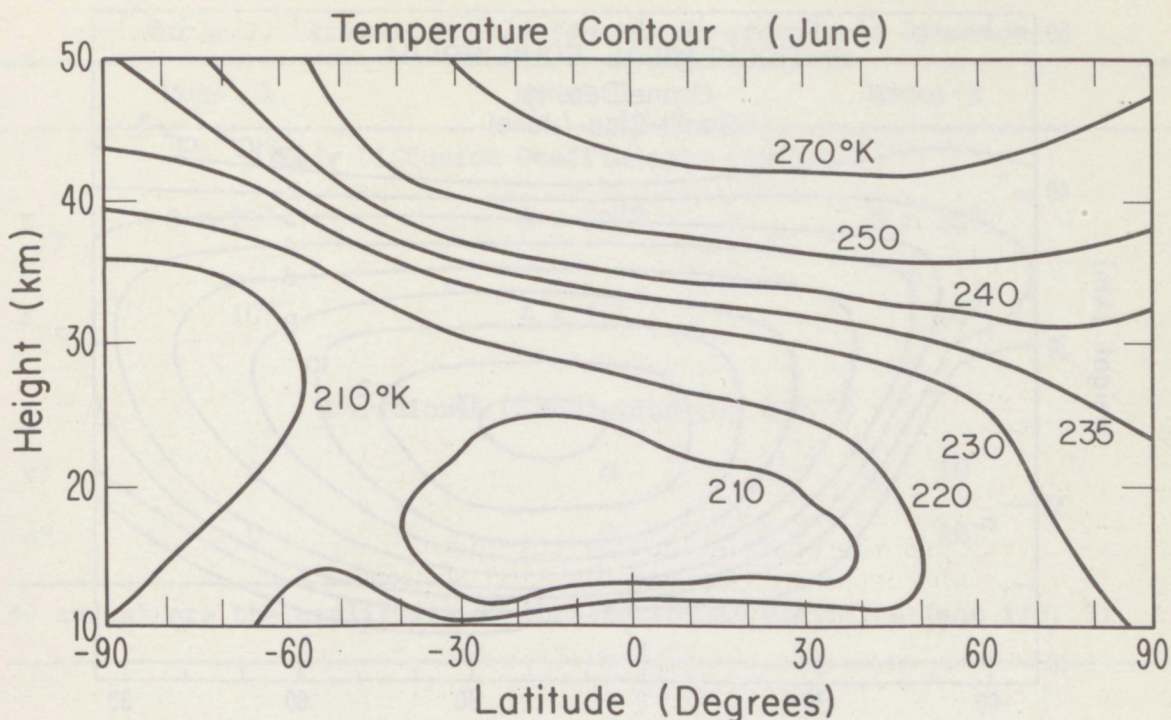


Figure 4. Contour map of constant temperature.

flux data and photodissociation cross-sections of O_2 and O_3 are taken from Ackerman (1971) and Hudson (1969). The reaction coefficients are based on Johnston (1968) for k_2 , and NBS Report 10828 (1972) for k_3 ; they are given by

$$k_2 = 4.65 \times 10^{-35} \exp(2100/RT) \quad (24)$$

and

$$k_3 = 2.0 \times 10^{-11} \exp(-4789/RT). \quad (25)$$

The result is shown in figure 5, which illustrates the contour map of the ozone density in the sunlit hemisphere for June. The overall maximum appears at the latitude slightly shifted towards the equator from the subpolar point ($23.5^\circ N$). The ozone density tends to decrease, while the height of the maximum increases with latitude. In particular, at high latitudes in winter, where the solar zenith angle approaches 90° , the

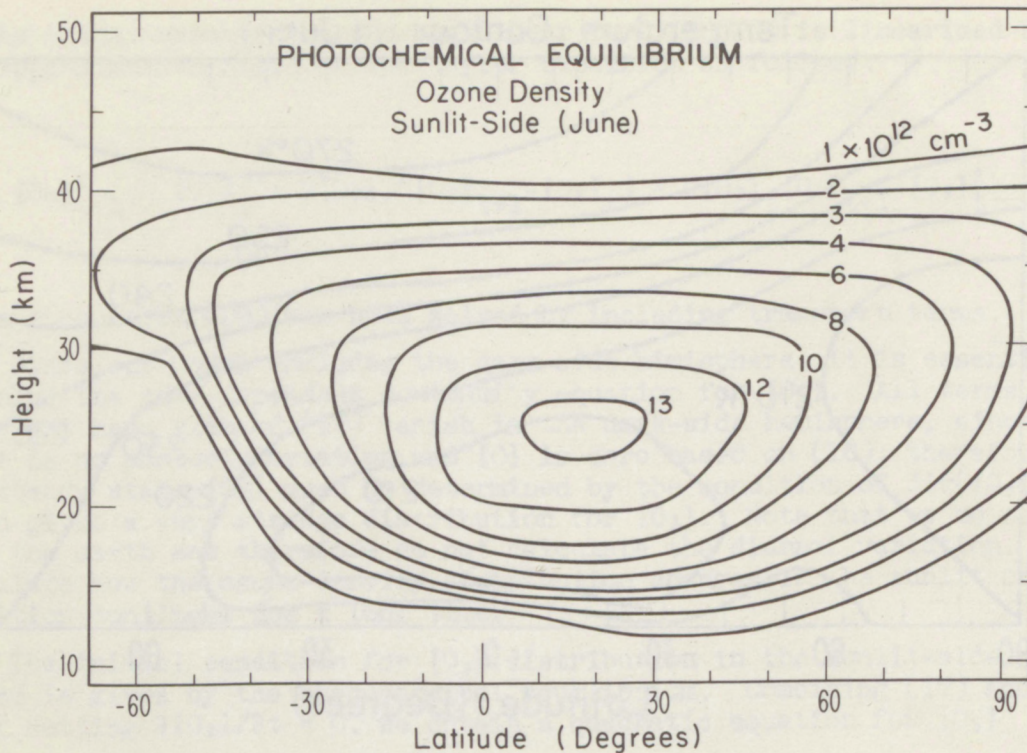


Figure 5. Contour map of $[O_3]$ of photochemical equilibrium model in sunlit-side hemisphere, June.

maximum $[O_3]$ occurs even above 35 km and the ozone density is very small below ~ 30 km. This is because the solar radiation needed for the production of O, the source of the formation of O_3 , has been absorbed at higher altitudes and does not reach below ~ 30 km.

6.2 Effects of Large Scale Eddy Diffusion

Using the photochemical equilibrium distribution calculated in the previous subsection as an initial condition, we have solved the continuity equation (20) as a time-dependent problem. Three models for the dynamics have been considered, as shown in Table 1. Models 1 and 2 assume the constant values for K's and neglect meridional circulation, while model 3 takes into account both eddy diffusion and meridional circulation. We discuss the effect of large scale eddy diffusion in this subsection.

Table 1. Assumed Models for the Stratospheric Dynamics

	Model 1	Model 2	Model 3
Eddy Diffusion Coefficients ($\text{cm}^2\text{sec}^{-1}$)			
K_{yy}	8×10^9	4×10^{10}	2×10^9
K_{zz}	10^4	4×10^4	10^3
Meridional Circulation (cm sec^{-1})			
v^*	0	0	10
w^*	0	0	10^{-2}

* v and w are the amplitudes of the sinusoidal variation (see fig. 3).

Model 2 assumes larger values for K 's than model 1, but there is no essential difference between the results of these two models. The result for model 1 is shown in figure 6(a) for the sunlit-side hemisphere and in figure 6(b) for the dark-side hemisphere. The calculation has been done for 300 model days.

In the sunlit-side hemisphere the chemical production and loss exist at all times, whereas in the dark-side hemisphere they exist just at the beginning (initial condition). These two cases corresponds to R3 and R2 models, respectively, of the experimental models of a stratospheric general circulation by Hunt and Manabe (1968). Their R2 model and our dark-side hemisphere model treat *an instantaneous source problem* and calculate the change from a photochemical equilibrium ozone density distribution by excluding any subsequent photochemistry. These models can isolate the dynamical effects from photochemical effects and may be useful in learning what the transport effects on the ozone density distribution are. The R3 model of Hunt and Manabe and our sunlit-side hemisphere model treat *a continuous source problem* and calculate a joint photochemical-dynamical effect with photochemistry incorporated at all times. These are useful to learn combined effects of the photochemistry and dynamics in maintaining the observed ozone density distribution.

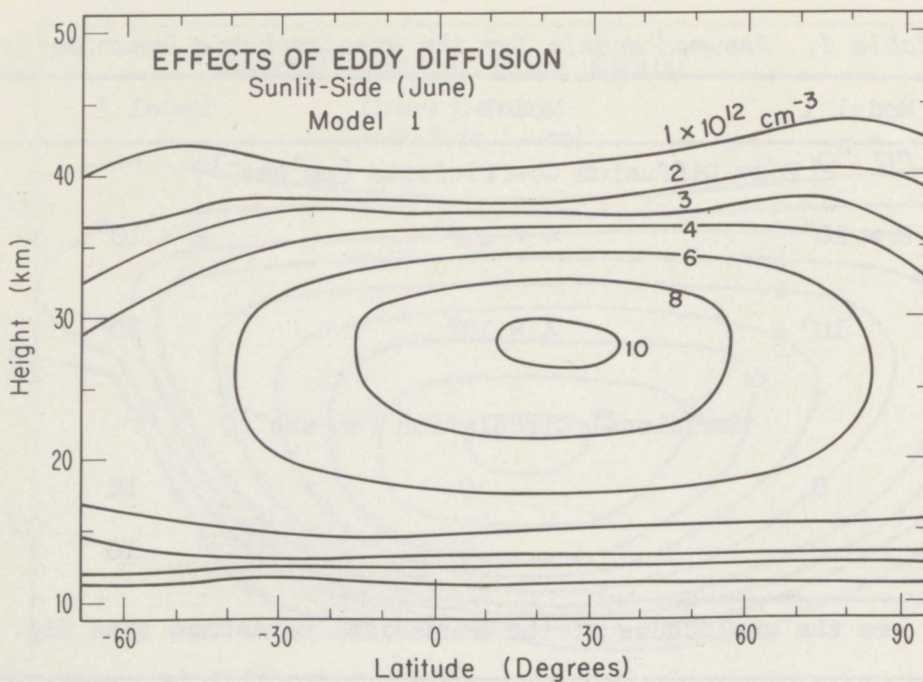


Figure 6(a). Contour map of $[O_3]$ of the model including effects of large scale eddy diffusion in the sun-lit-side hemisphere.

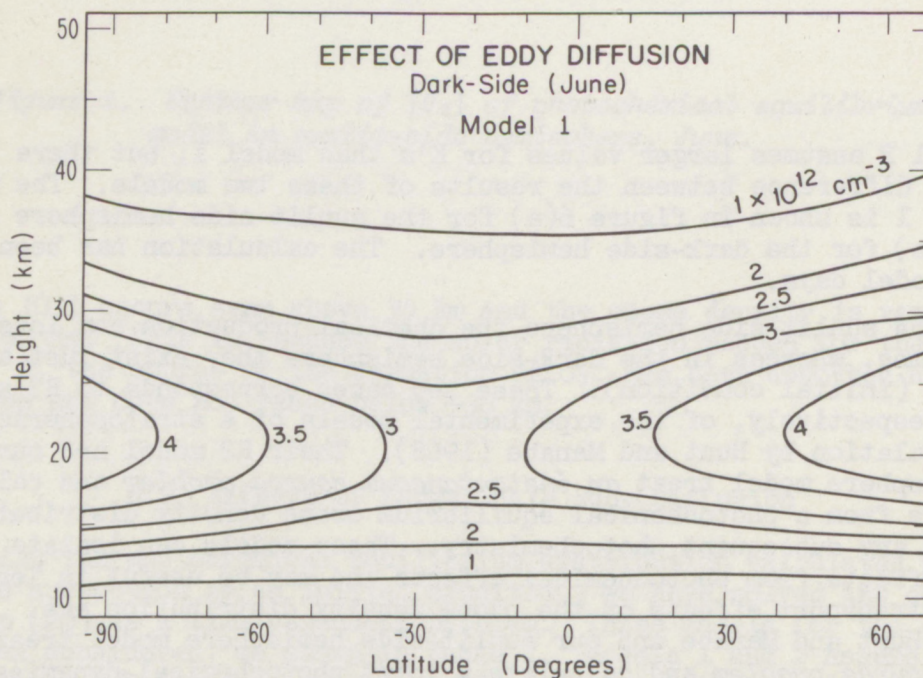


Figure 6(b). Contour map of $[O_3]$ of the model including effects of large scale eddy diffusion in the dark-side hemisphere.

Comparison of figure 6(a) with figure 5 reveals that the ozone density decreases at lower latitudes, while it increases at higher latitudes by the effect of diffusion. In particular, it is evident that at high latitudes in winter the ozone deficiency in the lower regions is filled by horizontal and vertical diffusion. It is also noted that the height of the maximum ozone density decreases markedly at high latitudes and is even lower than that at lower latitudes. These features agree well with the characteristics of the global distribution of the observed ozone density in the stratosphere.

Although effects of eddy diffusion look to be favorable in explaining the observations, the model still does not explain why the observed total ozone content increases with latitude. Figure 7(a) illustrates the latitudinal variation in the total ozone content and it is seen from the figure that both models 1 and 2 reduce a large maximum appearing in the initial (photochemical equilibrium) distribution, but that they do not change the general tendency of the latitudinal variation, i.e., the maximum still exists near the subsolar point, and the total content generally decreases with latitude. Obviously, this is against observations, a sample of which is taken from Dütsch (1971) shown in figure 7(a).

The result of the dark-side hemisphere of model 1 is shown in figure 6(b), in which the increase of the ozone density with latitude can clearly be seen. The same tendency can also be seen in figure 7(b), which illustrates the latitudinal variation in the total ozone content. The general tendency of the latitudinal variation now seems to agree with observations, but since there is not enough observational data for the nighttime ozone density, it is impossible to discuss the result quantitatively. Moreover, figure 6(b) does not represent any condition of real existence, since darkness has never been present continuously for such a long period *over the entire hemisphere*.

6.3 Effects of Eddy Diffusion Plus Meridional Circulation

It is evident from figure 7(a) that the effect of eddy diffusion alone can not explain the observed latitudinal variation in the total ozone content. Our model 3 considers the combined effects of eddy diffusion and meridional circulation.

In general, it is difficult to separate the possible effects of mean motions from those of eddy motions. Moreover, these two motions are known to have the opposite effects on $[O_3]$. The net effect should be caused by the difference between two large factors, divergence terms due to the two motions, and the residual should be much smaller than each of the two factors. Which of the two is larger depends upon season, latitude, local time, etc. It is too complicated to study in our model the details of these dependencies and their possible effects on the ozone density distribution.

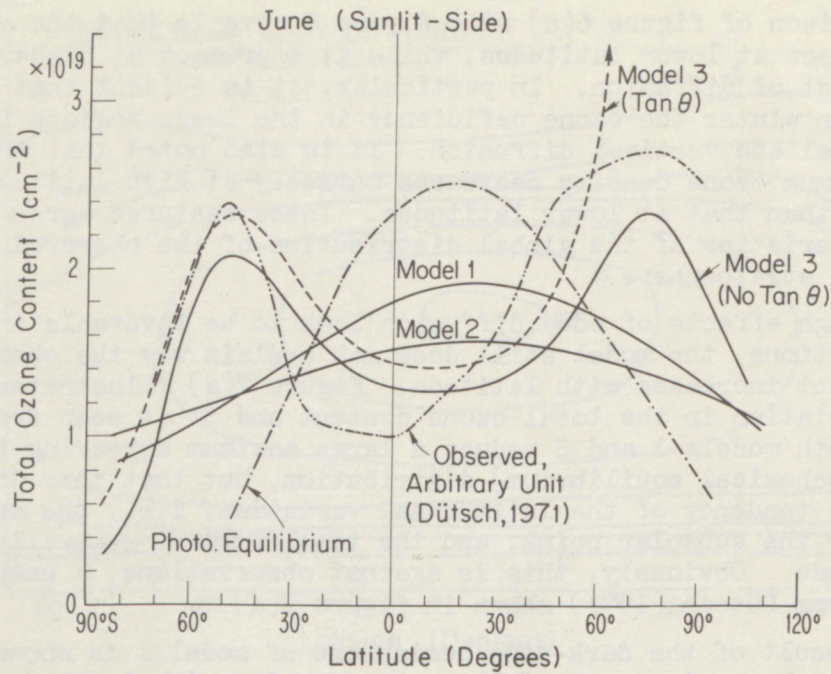


Figure 7(a). Latitudinal variation in the total ozone content (sunlit-side).

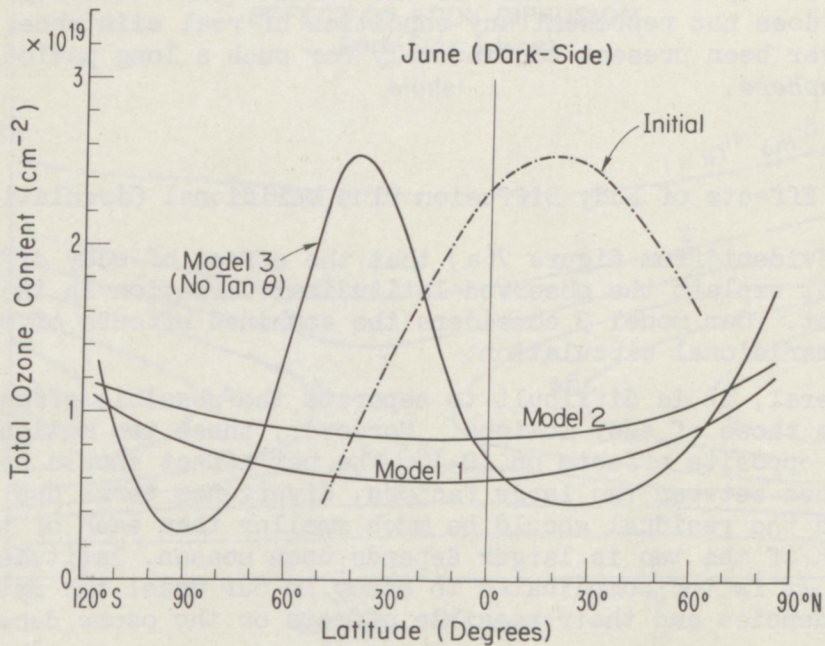


Figure 7(b). Latitudinal variation in the total ozone content (dark-side).

In model 3 we have adopted the values of K 's and velocity components of meridional circulation, which are almost an order of magnitude smaller than the usually accepted values, keeping in mind the fact that a large part of the effects of eddy diffusion and meridional circulation is cancelled out. K_{yy} and K_{zz} are usually considered to be on the order of 10^{10} and 10^4 $\text{cm}^2 \text{sec}^{-1}$, respectively. The horizontal and vertical components of mean meridional circulation velocity are usually estimated to be in an order of 10^2 and 10^{-1} cm sec^{-1} , respectively.

The result of the sunlit-side hemisphere of model 3 is shown in figure 8(a). The highest concentration now appears at high latitudes in both hemispheres. This is completely opposite to the distribution in photochemical equilibrium (see fig. 5), but agrees well with observations. The latitudinal variation of the total content of ozone also agrees well with observations seen in figure 7(a), except for the high latitudes in summer hemisphere. Since there is a poleward motion there at all longitudes in our model, the effect of convergence of the meridians represented by $\tan \theta$ terms in (1) and other forms of the continuity equation enhances greatly the ozone density towards the pole. Actually, however, such a convergence should be compensated by the counter flows, but this mechanism is not adequately taken into account in our zonally averaged model; therefore, it would be better to eliminate or reduce the effects of $\tan \theta$ terms in the present model. By so doing, we have a better agreement between the model result and observations, as is seen in figure 7(a). Our grid avoids the exact poles ($\theta = \pm 90^\circ$) by setting θ every 10° starting from $\pm 5^\circ$.

In the dark-side hemisphere, there is a large peak of the ozone density at middle latitudes in winter, as is seen in figure 7(b) and figure 8(b). It seems to be premature to discuss this peak, since the nighttime observations are scarce; however, theory suggests that there is not marked diurnal variation in $[O_3]$ in the stratosphere, and the existence of this large peak at the winter middle latitude seems to be hard to explain. Thus, the result may suggest that meridional circulation is weaker in the dark-side hemisphere than in the sunlit-side hemisphere.

Figure 9 illustrates the rate of the change in $[O_3]$ caused by eddy diffusion and meridional circulation at various latitudes in both sunlit-side and dark-side hemispheres. As is expected, it is clearly seen that these two rates compete with each other; they have opposite signs with almost the same magnitude. The pattern of the latitudinal variation in figure 9 should depend upon the pattern of the cell motions assumed in figure 3.

One of the advantages of our modeling technique was that we did not need to assume the zero-flux boundary conditions at poles and equators. These fluxes calculated in our model 3 is shown in figure 10. At the equator in the dark-side hemisphere the flux caused by meridional circulation and eddy diffusion is almost cancelled out, but at the equator in the sunlit-side hemisphere there is a net flux from the summer to winter hemisphere in regions above ~ 30 km. At poles there is no flux due to meridional circulation in our model (see fig. 3), and the flux due to eddy diffusion is directed from sunlit-side to dark-side hemisphere at all heights at the summer pole and in regions above ~ 30 km at the winter pole. There is a flow from the dark- to sunlit-side in lower regions at the winter pole.

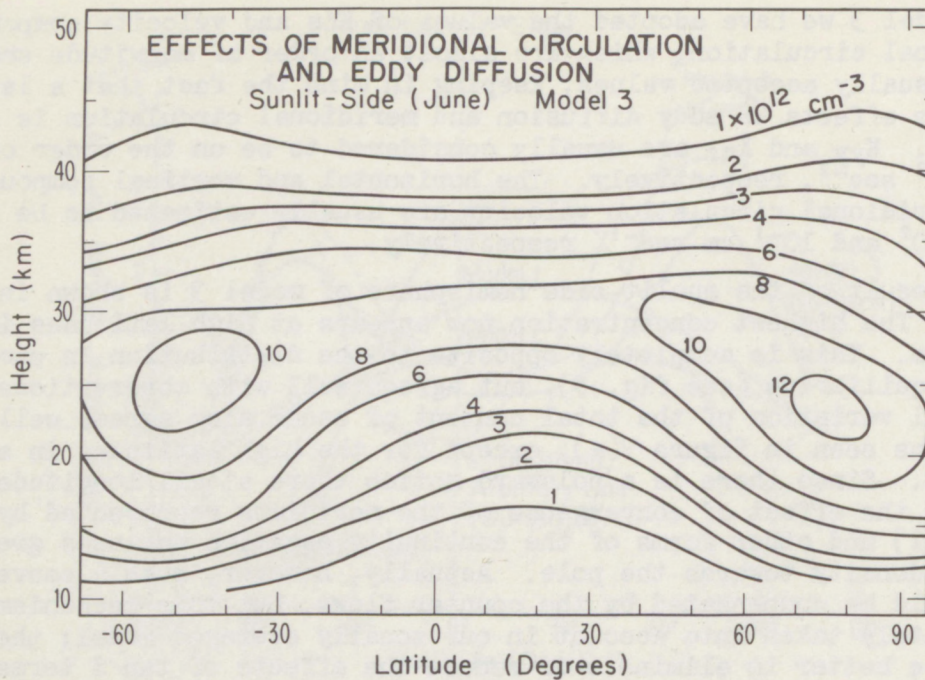


Figure 8(a). Contour map of $[O_3]$ of the model including combined effects of large scale eddy diffusion and meridional circulation in sunlit-side hemisphere.

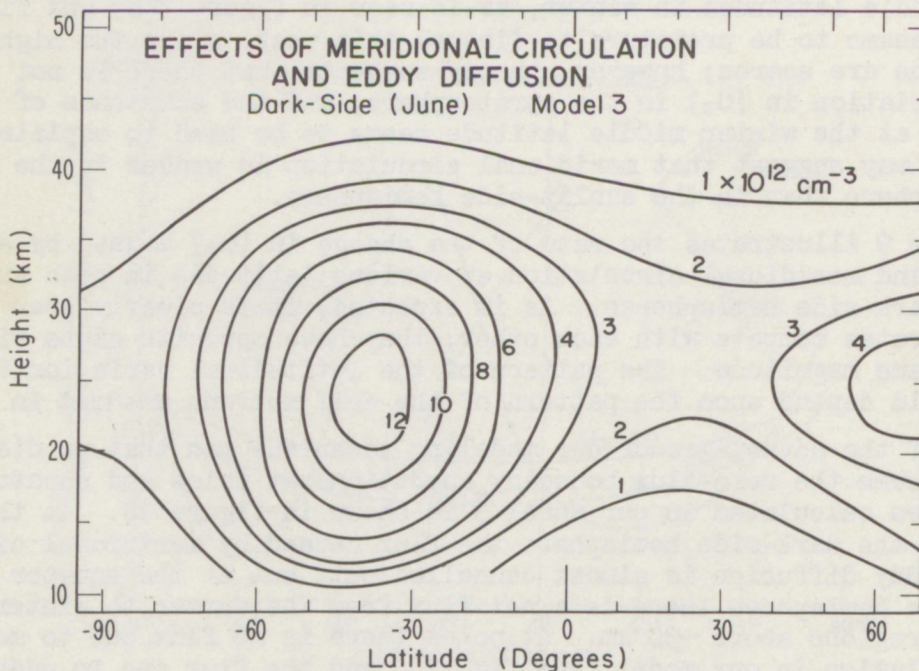


Figure 8(b). Contour map of $[O_3]$ of the model including combined effects of large scale eddy diffusion and meridional circulation in dark-side hemisphere.

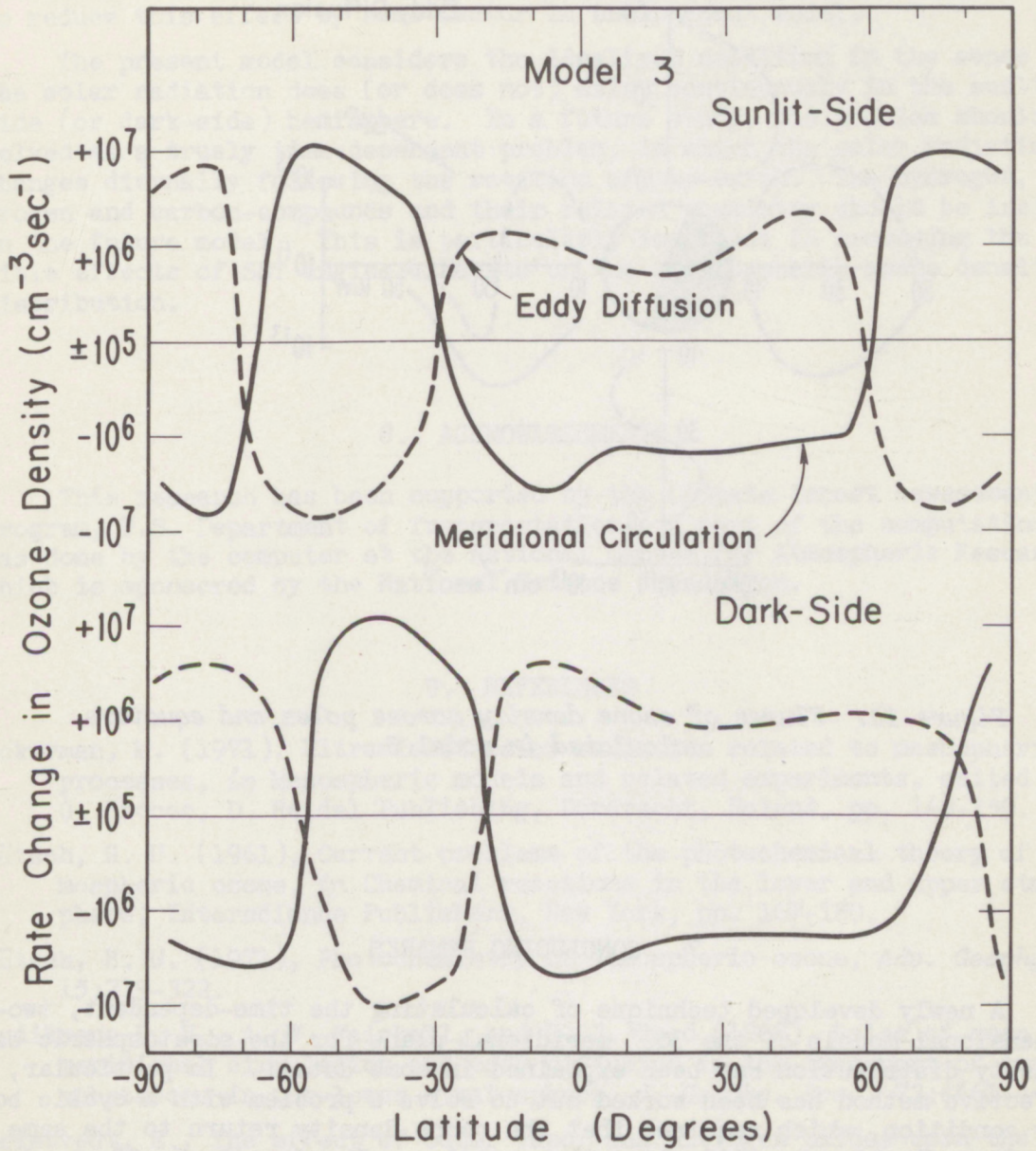


Figure 9. Rate of change in $[O_3]$ due to large scale eddy diffusion and meridional circulation at various latitudes.

FLUXES AT POLES AND EQUATORS

MODEL 3

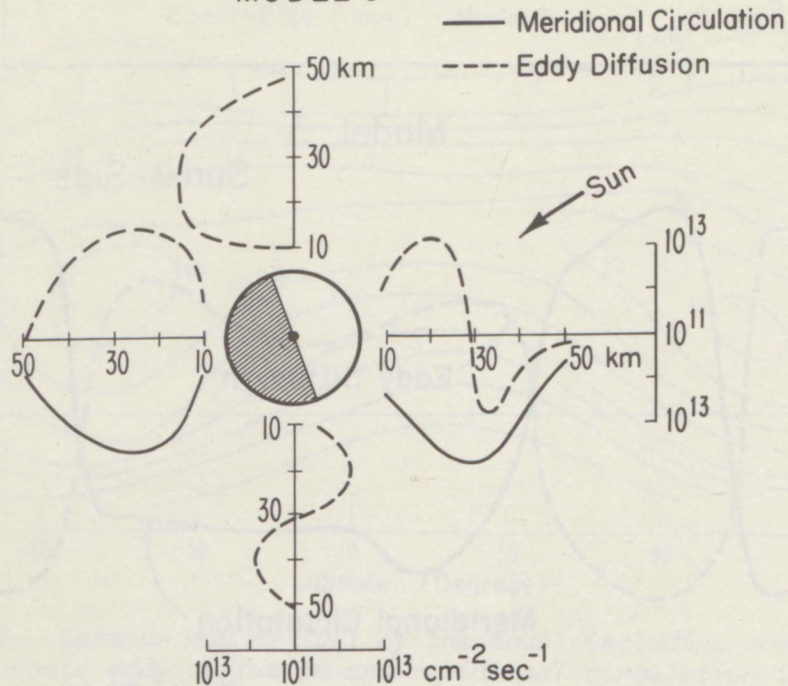


Figure 10. Fluxes of ozone density across poles and equators calculated in model 3.

7. CONCLUDING REMARKS

A newly developed technique of calculating the time-dependent, two-dimensional models of the 360° meridional plane for the stratospheric ozone density distribution has been explained in some detail. In particular, an effective method has been worked out to solve a problem with a cyclic boundary condition, which requires that the ozone density return to the same value after circling by 360° along the meridian. The dynamical effects due to large scale eddy motions and meridional circulations, as well as ozone chemistry, are incorporated in the model. The dynamics are included by way of parameterization and do not represent the real dynamics, but their effects on the global distribution of the ozone density are very noticeable and are favorable for explaining the observations, which indicate tendencies of increasing density and lowering the height of the peak density with increasing latitude. The photochemical equilibrium model had displayed tendencies in the entirely opposite direction.

The zonal average model calculated in this study can not treat adequately the effects of convergence of the meridians towards the poles; they produced a largely enhanced ozone density at high latitudes when poleward motion occurred in the meridional circulation. Therefore, it seems wise to reduce this effect by some factor in the present model.

The present model considers the idealized condition in the sense that the solar radiation does (or does not) exist continuously in the sunlit-side (or dark-side) hemisphere. In a future study, the problem should be solved as a truly time-dependent problem, in which the solar radiation changes diurnally following the rotation of the earth. The hydrogen, nitrogen and carbon-compounds and their related chemistry should be included in the future model. This is particularly important in assessing the possible effects of SST engine exhausts on the stratospheric ozone density distribution.

8. ACKNOWLEDGMENTS

This research has been supported by the Climate Impact Assessment Program, U.S. Department of Transportation. A part of the computation was done by the computer at the National Center for Atmospheric Research, which is sponsored by the National Science Foundation.

9. REFERENCES

- Ackerman, M. (1971), Ultraviolet solar radiation related to mesospheric processes, *in* Mesospheric models and related experiments, edited by G. Fiocco, D. Reidel Publishing, Dordrecht, Holand, pp. 149-159.
- Dütsch, H. U. (1961), Current problems of the photochemical theory of atmospheric ozone, *in* Chemical reactions in the lower and upper atmosphere, Interscience Publishers, New York, pp. 167-180.
- Dütsch, H. U. (1971), Photochemistry of atmospheric ozone, *Adv. Geophy.* 15:219-322.
- Gudiksen, P. H., A. W. Fairhall, and R. J. Reed (1968), Roles of mean meridional circulation and eddy diffusion in the transport of trace substances in the lower stratosphere, *J. Geophy. Res.*, 73:4461-4473.
- Hesstvedt, E., The effect of water vapor and nitrogen oxides upon the ozone layer, studies in a photochemical model with meridional transport, in press *in* Pure and Applied Geophysics.
- Hudson, R. D., V. L. Carter, and E. L. Brieg (1969), Predissociation in the Schumann-Runge band system of O₂: Laboratory measurements and atmospheric effects, *J. Geophys. Res.*, 74:4079-4086.

- Hunt, B. G., and S. Manabe (1968), Experiments with stratospheric general circulation model, *Monthly Weather Review*, 96(8):503-539.
- Jacobi, W., and K. André (1963), The vertical distribution of radon 222, radon 220, and their decay products in the atmosphere, *J. Geophys. Soc.* 68:3799-3814.
- Johnston, H. (1968), Gas phase reaction kinetics of neutral oxygen species, National Standard Reference Data Series, NBS 20.
- Murgatroyd, R. J. (1957), Winds and temperatures between 20 km and 100 km - a review, *Quart. J. Royal Meteor. Soc.*, 83:417-458.
- NBS Report 10828 (1972), Chemical kinetics data survey, II. Photochemical and rate data for fifteen gas phase reactions of interest for stratospheric chemistry.
- Nicolet, M. (1972), Aeronomic chemistry of the stratosphere, *Aeronomica Acta*, A-N96, Institute D'Aeronomie Spatiale de Belgique, Bruxelles.
- Prabhakara, C. (1963), Effects of non-photochemical processes on the meridional distribution and total amount of ozone in the atmosphere, *Monthly Weather Rev.*, 91:411-430.
- Reed, R. J., and K. E. German (1965), A contribution to the problem of stratospheric diffusion by large-scale mixing, *Monthly Weather Review*, 93:313-321.
- Richtmyer, R. D., and K. W. Morton (1967), Difference methods for initial-value problems, Interscience Publisher, New York.
- Shimazaki, T. (1967), Dynamic effects on atomic and molecular oxygen density distributions in the upper atmosphere: A numerical solution to equations of motion and continuity, *J. Atmosph. Terr. Phy.*, 29:723-747.
- Shimazaki, T. (1972), On the boundary conditions in theoretical model calculations of the distributions of minor neutral constituents in the upper atmosphere, *Radio Science*, 7:695-702.
- Shimazaki, T., and A. R. Laird (1970), A model calculation of the diurnal variation in minor neutral constituents in the mesosphere and lower thermosphere including transport effects, *J. Geophys. Res.* 75:3221-3235, (see also 77:276-277, 1972).
- Shimazaki, T., and A. R. Laird (1972), Seasonal effects on distributions of minor neutral constituents in the mesosphere and lower thermosphere, *Radio Science*, 7:23-43.
- Vincent, D. G. (1968), Mean meridional circulations in the northern hemisphere lower stratosphere during 1964 and 1965, *Quart. J. Roy. Met. Soc.*, 94:333-349.
- Young, D. M. (1962), The numerical solution of elliptic and parabolic partial differential equations, in *Survey of numerical analysis*, edited by J. Todd, McGraw-Hill Book Company, New York, pp. 380-438.

APPENDIX 1: AN IMPLICIT METHOD FOR THE COLUMN j

Equation (3) in the text can be written in a form

$$- A \cdot n^{\ell+1}(j, k+1) + B \cdot n^{\ell+1}(j, k) - C \cdot n^{\ell+1}(j, k-1) = D \quad (\text{A-1})$$

where A, B, C, and D are functions of known variables at the time ℓ and are the simplified expressions of $A^\ell(j, k)$ etc. D also includes a function of $n^\ell(j-1, k)$, $n^\ell(j, k)$ and $n^\ell(j+1, k)$.

Putting

$$n^{\ell+1}(j, k) = E^\ell(j, k) \cdot n^{\ell+1}(j, k+1) + F^\ell(j, k) \quad (\text{A-2})$$

and the substitution of (A-2) and the similar equation for $n^{\ell+1}(j, k-1)$ into (A-1) gives the following recurrence formula for E and F. (We omit the subscript j and the superscript ℓ in the following equations.)

$$E(k) = \frac{A(k)}{B(k) - C(k) \cdot E(k-1)} \quad , \quad F(k) = \frac{D(k) + C(k) \cdot F(k-1)}{B(k) - C(k) \cdot E(k-1)} \quad (\text{A-3})$$

Consideration of (A-2) at the lower boundary $k=1$ leads to

$$E(1) = 0, \quad F(1) = n^{\ell+1}(1). \quad (\text{A-4})$$

Since we have assumed a constant vertical flux with height at the lower boundary, neglecting the effect of horizontal divergence at the lower boundary we can calculate $n^{\ell+1}(1)$ by (Shimazaki, 1972)

$$n^{\ell+1}(1) = \frac{n^\ell(1) + Q^\ell(1) \Delta t}{1 + L^\ell(1) \Delta t} \quad (\text{A-5})$$

Thus, $E(k)$ and $F(k)$ can be calculated by (A-3) inductively in order of increasing k from the values at $k=1$ given by (A-4) and (A-5).

At the upper boundary photochemical equilibrium is assumed for O_3 ; therefore, $n^{\ell+1}(K)$ can be calculated by (23) in the text. We then calculate $n^{\ell+1}(k)$ for all k by (A-2) inductively in order of decreasing k.

APPENDIX 2: AN IMPLICIT METHOD FOR THE ROW k
(CYCLIC BOUNDARY CONDITION)

In any model of global scale, if we consider a part of the entire region of the atmosphere as a domain, a boundary condition is needed at the boundary between that domain and the rest of the region. The boundary condition should be determined by the interaction between the two regions, and we have to know the physical and chemical conditions in the outside as well as in the inside of the boundary in order to specify the boundary condition.

It would be better to include the entire region in the domain in the global scale modeling. Then, the boundary condition can be given simply by the requirement of the cyclic variation, i.e., any variable should have the same value every 360° or after a complete rotation on the earth. In case of solving the continuity equation for $[O_3]$, if we divide a 360° meridional plane into J division, the boundary condition requires that $[O_3]$ should be the same at $j=1$ and $j=J$.

Equation (9) in the text can be written in a form of

$$- A \cdot n^{\ell+1}(j+1,k) + B \cdot n^{\ell+1}(j,k) - C \cdot n^{\ell+1}(j-1,k) = D \quad (A-6)$$

where A , B , C , and D are functions of known variables at the time ℓ and are the simplified expressions of $A^\ell(j,k)$ etc. D also includes a function of $n^\ell(j,k+1)$, $n^\ell(j,k)$ and $n^\ell(j,k-1)$. A , B , C , and D in (A-6) are not necessary to be the same as those in (A-1).

By the treatment similar to that in Appendix 1, writing

$$n^{\ell+1}(j,k) = E^\ell(j,k) \cdot n^{\ell+1}(j+1,k) + F^\ell(j,k) \quad (A-7)$$

we obtain the following recurrence formulae for E and F (we omit the subscript k and the superscript ℓ in the following equations)

$$E(j) = \frac{A(j)}{B(j) - C(j) \cdot E(j-1)}, \quad F(j) = \frac{D(j) + C(j) \cdot F(j-1)}{B(j) - C(j) \cdot E(j-1)}. \quad (A-8)$$

We first calculate a special solution for $E(j)$ and $F(j)$ assuming

$$E(1) = 0, \text{ and } F(1) = n^\ell(1) \quad (A-9)$$

and using (A-8) inductively in order of increasing j .

At $j=J$ we have

$$n^{\ell+1}(J) = E(J) \cdot n^{\ell+1}(J+1) + F(J). \quad (A-10)$$

Because of the cyclic variation for $n(j)$, this should be equivalent to

$$n^{\ell+1}(1) = E(1) \cdot n^{\ell+1}(2) + F(1). \quad (A-11)$$

Therefore, we now have the revised values for $E(1)$ and $F(1)$, which should be equal to $E(J)$ and $F(J)$ in (A-10), respectively, and should replace the starting condition given by (A-9). Thus, repeating the same procedure we recalculate $E(j)$ and $F(j)$ by (A-8). The result should not be too much different from the result of the previous calculation starting from (A-9).

Using (A-7) repeatedly, we have

$$\begin{aligned} n^{\ell+1}(1) &= E(1) \cdot E(2) \cdot E(3) \dots E(J-2) \cdot E(J-1) \cdot n^{\ell+1}(J) \\ &+ E(1) \cdot E(2) \cdot E(3) \dots E(J-2) \cdot F(J-1) \\ &+ E(1) \cdot E(2) \dots E(J-3) \cdot F(J-2) \\ &+ \dots \\ &+ \dots \\ &+ E(1) \cdot E(2) \cdot F(3) \\ &+ E(1) \cdot F(2) \\ &+ F(1) . \end{aligned} \quad (A-12)$$

Since the cyclic boundary condition required that $n(1) = n(J)$, the above equation can be solved for $n^{\ell+1}(J)$ as follows:

$$n^{\ell+1}(J) = \frac{F(1) + \sum_{j=3}^J E(1) \cdot E(2) \dots E(j-2) \cdot F(j-1)}{1 - E(1) \cdot E(2) \dots E(J-1)} . \quad (A-13)$$

Actually, the summation in the numerator of the right hand side of (A-13) can be determined by the first several terms, since $E(j)$ is generally smaller than unity. $n^{\ell+1}(j)$ are now calculated for all j by (A-7) inductively in order of decreasing j using the recalculated $E(j)$ and $F(j)$ and $n^{\ell+1}(J)$ calculated from (A-13).